AFRL-RZ-WP-TP-2007-246

A DETAILED INVESTIGATION OF BLUFF BODY STABILIZED FLAMES (POSTPRINT)

Barry Kiel, Lt. Kyle Garwick, Dr. James R. Gord, Joseph Miller, and Amy Lynch

Combustion Branch
Turbine Engine Division

AUGUST 2007

Approved for public release; distribution unlimited.
See additional restrictions described on inside pages

STINFO COPY

AIR FORCE RESEARCH LABORATORY
PROPULSION DIRECTORATE
WRIGHT-PATTERSON AIR FORCE BASE, OH 45433-7251
AIR FORCE MATERIEL COMMAND
UNITED STATES AIR FORCE

REPORT DOCUMENTATION PAGE	*Form Approved OMB No. 0704-0188*

1. REPORT DATE ***(DD-MM-YY)***	**2. REPORT TYPE**	**3. DATES COVERED *(From - To)***
August 2007	Conference Paper Postprint	01 August 2005 – 01 August 2007

4. TITLE AND SUBTITLE

A DETAILED INVESTIGATION OF BLUFF BODY STABILIZED FLAMES (POSTPRINT)

5a. CONTRACT NUMBER In-house

5b. GRANT NUMBER

5c. PROGRAM ELEMENT NUMBER 62203F

6. AUTHOR(S)

Barry Kiel, Lt. Kyle Garwick, Dr. James R. Gord, Joseph Miller, and Amy Lynch (AFRL/RZTC)
Dr. Roger Hill and Dr. Scott Phillips (Creare Incorporated)

5d. PROJECT NUMBER 3066

5e. TASK NUMBER 05

5f. WORK UNIT NUMBER 306605YY

7. PERFORMING ORGANIZATION NAME(S) AND ADDRESS(ES)

Combustion Branch (AFRL/RZTC), Turbine Engine Division
Air Force Research Laboratory, Propulsion Directorate
Wright-Patterson Air Force Base, OH 45433-7251
Air Force Materiel Command, United States Air Force

Creare Incorporated
P.O. Box 71
Hanover, NH 03755

8. PERFORMING ORGANIZATION REPORT NUMBER

AFRL-RZ-WP-TP-2007-246

9. SPONSORING/MONITORING AGENCY NAME(S) AND ADDRESS(ES)

Air Force Research Laboratory
Propulsion Directorate
Wright-Patterson Air Force Base, OH 45433-7251
Air Force Materiel Command
United States Air Force

10. SPONSORING/MONITORING AGENCY ACRONYM(S)

AFRL/RZTC

11. SPONSORING/MONITORING AGENCY REPORT NUMBER(S)

AFRL-RZ-WP-TP-2007-246

12. DISTRIBUTION/AVAILABILITY STATEMENT

Approved for public release; distribution unlimited.

13. SUPPLEMENTARY NOTES

Conference paper published in the Proceedings of the 45th AIAA Aerospace Sciences Meeting and Exhibit.

The U.S. Government is joint author of this work and has the right to use, modify, reproduce, release, perform, display, or disclose the work.

PAO Case Number: AFRL/WS 06-2928, 18 Dec 2006.

14. ABSTRACT

Reduced Order Models (ROMs) and Computational Fluid Dynamics (CFD) codes are tools used to predict the extinction of flames behind bluff bodies. Accurate prediction of these models and codes is predicated on their validation with experimental data. This paper describes detailed experiments to obtain validation data for bluff body stabilized flames over a wide range of conditions. Included are non-reacting data from CFD and LDV, lean blowout and high speed images for three different flame holders. In our previous paper (Kiel 2006) it was asserted that the large vortices were a major driver of extinction. Those assertions are further supported here. It is concluded that the vortex dynamics and not geometry is the dominant mechanism for bluff body flame extinction. This conclusion is supported by the lean blowout data, by the high speed images and reference data from NACA.

15. SUBJECT TERMS

16. SECURITY CLASSIFICATION OF:			**17. LIMITATION OF ABSTRACT:**	**18. NUMBER OF PAGES**	**19a. NAME OF RESPONSIBLE PERSON** (Monitor)
a. REPORT	**b. ABSTRACT**	**c. THIS PAGE**			Lt. Kyle Garwick
Unclassified	Unclassified	Unclassified	SAR	16	**19b. TELEPHONE NUMBER** *(Include Area Code)* N/A

Standard Form 298 (Rev. 8-98)
Prescribed by ANSI Std. Z39-18

2007 AIAA Aerospace Sciences Meeting and Exhibit AIAA 2007-0168
8-11 January, 2007, Reno NV.

A Detailed Investigation of Bluff Body Stabilized Flames

Barry Kiel, Kyle Garwick, Dr James R. Gord, and Joseph Miller, and Amy Lynch
Air Force Research Laboratory
Wright Patterson Air Force Base

Dr. Roger Hill and Dr. Scott Phillips
Creare Inc.
Hanover, New Hampshire

ABSTRACT

Reduced Order Models (ROMs) and Computational Fluid Dynamics (CFD) codes are tools used to predict the extinction of flames behind bluff bodies. Accurate prediction of these models and codes is predicated on their validation with experimental data. This paper describes detailed experiments to obtain validation data for bluff body stabilized flames over a wide range of conditions. Included are non-reacting data from CFD and LDV, lean blowout and high speed images for three different flame holders

In our previous paper (Kiel 2006) it was asserted that the large vortices were a major driver of extinction. Those assertions are further supported here. It is concluded that the vortex dynamics and not geometry is the dominant mechanism for bluff body flame extinction. This conclusion is supported by the lean blowout data, by the high speed images and reference data from NACA.

NOMENCLATURE

CFD	Computational Fluid Dynamics
FFT	Fast Fourier Transform
DNS	Direct Numerical Simulation
k	wave number
L	v-gutter length scale
LES	Large Eddy Simulation
LDV	Laser Doppler Velocimetry
URANS	Un-steady Reynolds Averaged Navier Stokes
Re	Reynolds Number
rms	root mean square
St	Strouhal Number
U	velocity
ω	frequency

1 INTRODUCTION

Integral to any combustion system is it's extinction performance over the operating range of the combustion system. For bluff body stabilized flames vortex motion is seen as a key driver to the stability of the flame. For the past fifty years bluff body stabilized flames have been studied in detail. In the 1950s DeZubay (1950) and King (1957), studied flames stabilized using bluff bodies. Both authors found that the fuel air ratio the flame blows out at correlates with the inlet pressure, temperature, and velocity. Also in the 1950's Zukoski (1954, 1955) studied blowout of bluff body flames. Zukoski found that the blow out characteristics behave quite differently at lower Reynolds numbers. Zukoski concluded that the flame transitions from "laminar" to "turbulent" around a Reynolds numbers of 10,000. Later Ozawa (1971) also compiled data from several bluff body experiments. Ozawa also discusses this blowout transition at Reynolds Number of 10,000. Both authors conclude the flame surface transitions from "laminar" to "turbulent" near this Reynolds number. Further, they both concluded that this transition greatly effects the velocity at which the flame will blow off at, or the characteristic of the blow-out curve.

More recently Mehta and Soteriou (2003), and Erickson et al. (2006) have commented on vortex shedding as it relates to bluff body flame blow-out. I their work they have conducted detailed modeling of bluff body stabilized flames. In their 2003 work they concluded that the baroclinic effect of the temperature rise across the flame suppresses the Karman Street type vortex shedding typically seen behind these bluff bodies under non-combusting conditions. In this paper they modeled a bluff body flame at 20,000 Reynolds number. They concluded that the flame was dominated not by large Karman Street vortices but much smaller vortices. They also concluded that the baroclinic torque generated by the temperature rise across the flame was responsible for suppressing the Karma Street vortex production.

Later in 2006, (Ericson et al. (2006)) they conducted another model study where the temperature rise across the flame was varied. In this study they concluded that at lower temperature ratios across the flame, the flame near blowout was dominated not by small turbulent vortices but by large Karman Street type vortices. These same structures were also captured by Porumbel and Menon (2006), and Fureby (2006) in their combusting Large Eddy Simulation (LES) investigations.

This paper is the second in a series of experimental papers where bluff body flames in cross flow are studied in detail. In this paper three bluff bodies are examine; a v-gutter, a circular cylinder and a square “cylinder”. For each bluff body the dimensionless vortex shedding in non-combusting flow is reported from various sources. Also reported are detailed lean blow out measurements taken over a wide range of inlet velocities. High speed images of each flame holder were also taken at equivalence rations near stoichiometric and near blow out. The images for the two different equivalence rations and flame holders are compared and contrast. Finally in this paper URANS calculations for the “closed” v-gutter flame holder were conducted using the Fluent CFD solver. The CFD results are compared to previously reported Laser Doppler Velocimetry (LDV) data.

2 HIGH SPEED IMAGING PROCEDURES

Movies of the turbulent flame structure behind a bluff body were captured using a Phantom v7.1 high speed camera from Vision Research. The Phantom v7.1 is a 12 bit SR-CMOS monochrome camera with a Gigabit Ethernet connection capable of capturing video at a max resolution of 800 x 600 pixels at 4800 frames-per-second (fps), or images at a smaller resolution up to a 160,000 fps. Simultaneous top and side-view images were collected at a resolution of 576 x 376 pixels with a frame rate of 5000 and 7500 fps using a 50mm focusing lens at an f-stop of 2.8. Exposure times ranged from 180us to 120us, respectively. On average, 2000 images were collected at each test condition for multiple bluff body configurations.

3 EXPERIMENTAL SETUP

A 12MW experimental combustion facilities located at the Propulsion Directorate of AFRL in Wright-Patterson Air Force Base, Dayton Ohio was used for the experiments. Figure 3-1 is a schematic of the experimental rig with the v-gutter bluff body flame holder installed. Experiments were also conducted with a circular cylinder and a square cylinder, Figure 3-2. Each flame holder had a width of 1.5 inches. In these experiments the flame holder traverses the length of the test section. In this configuration the flow is considered two-dimensional at the center of the test rig.

4 NON-REACTING FLUID DYNAMICS DATA

4.1 Dimensionless Vortex Shedding

Previously, extensive LDV were conducted on the v-gutter configuration (Kiel 2006). Subsequent data for different bluff body geometries from other authors has been compiled with the v-gutter, (Roskko 1954a, 1954b, Blevins 1985, Blevins, 1977, Younger et al . 1951, Norburg 1993, Taylor and Vezza 1999). Figure 4-1 is a plot of experiments LDV data and data from other authors. For the three flame holder geometries investigated the shedding frequencies in isothermal non-reacting flow are quite different. When the three sets of dada fro each of the flame holders are compared several things can be concluded.

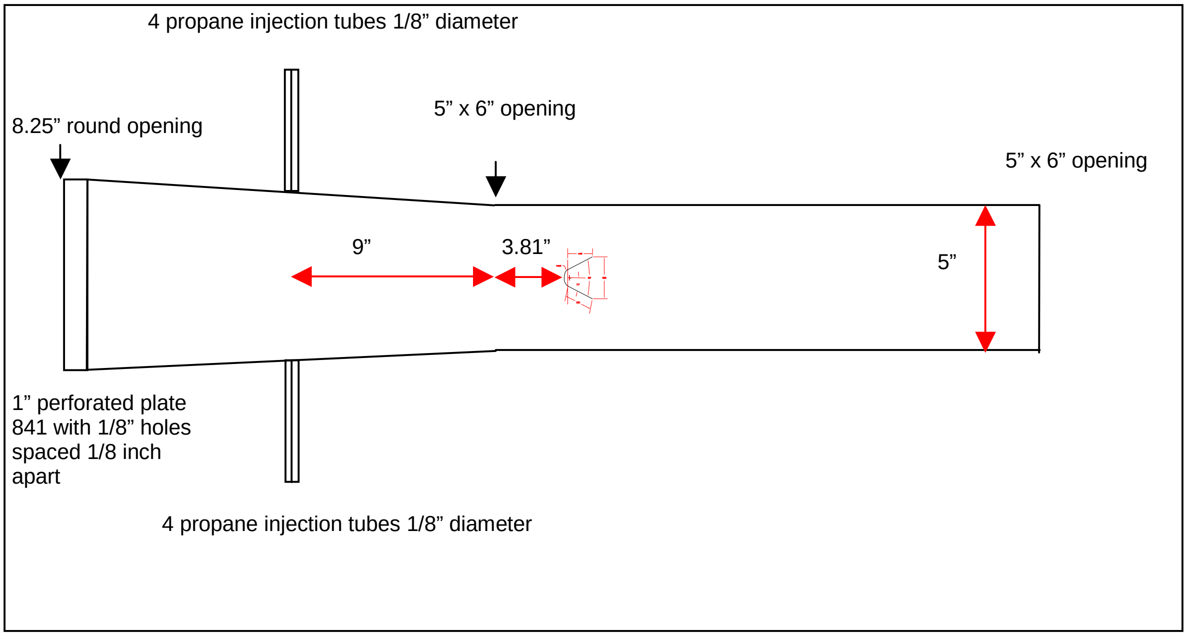

Figure 3-1 Experimental Apparatus, Pictured with V-Gutter Installed

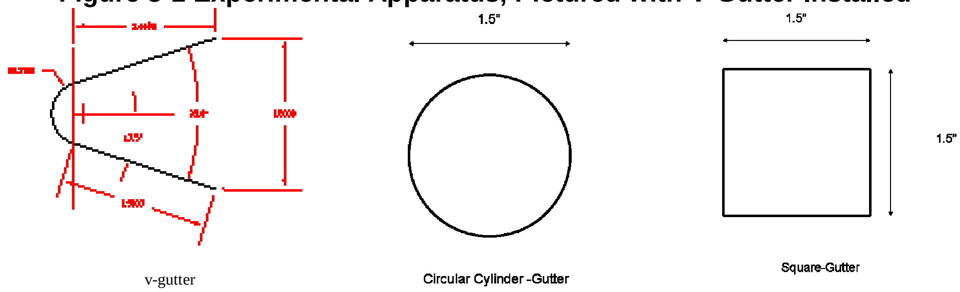

Figure 3-2 V-gutter, Circular and Square Cylinder Bluff Body Flame Holder Geometry

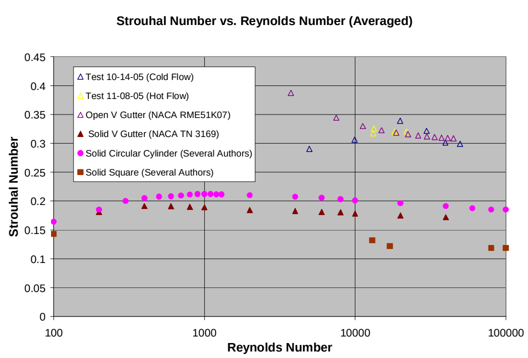

Figure 4-1. Dimensionless Shedding Frequency Several Reynolds Numbers

Over the range of Reynolds numbers studied each of the bluff bodies has different frequencies at which vortices are shed. For the circular cylinder the dimensionless frequency is approximately 0.21. For the v-gutter the shedding frequencies were approximately 0.31. For the square cylinder the shedding frequency is 0.13. For the range of inlet Reynolds number’s investigated the Strouhal number does not exhibit substantial changes. Sufficient data do not exist to make a more detailed comparison of the v-gutter and circular cylinder vortex shedding to the square cylinder.

4.2 Comparison of Mean and rms Experimental Data to CFD

Non-reacting simulations were also conducted using the commercially available Fluent CFD code. The problem was set up using the Unsteady Reynolds Averaged Navier Stokes (URANS) option. The inlet boundaries were modeled with experimentally measured velocity and turbulence profiles. At the exit constant pressure was assumed. Two different turbulence models were used in the analysis, the k-epsilon and realizable turbulence models.

Figures 4-2 to 4-4 depicts the Fluent URANS simulation with the k-epsilon turbulence model and the experimental LDV data (Kiel 2006). Each plot is a traverse across the wake of the flame holder. On the left are traverses of the mean and rms axial velocity. On the right are traverses of the mean and rms transverse velocity. For each plot the y axis was non-dimensionalized by the flame holder dimension, 1.5 inches, and the x-axis was non-dimensionalized by the bulk inlet velocity.

The simulation had mixed success when compared to the experimental data. In all three cases the k-epsilon compares reasonable well in the portion of the flow that is outside the wake of the flame holder. For all of the traverses the mean and rms velocity compared to within less than 2%.

In the wake region the simulation did not fare as well. For the axial component of velocity the simulation captured the correct trend of the rms velocity but over predicted the magnitude of the rms routinely by 50%. For the mean velocity in the wake, the simulation predicted the location of the shear layer closer to the center line of the flame holder than the experiment. For the transverse component of velocity the simulation predicted the rms velocity very well in the wake region, but over predicted the rms in the region of the shear layer. In all cases transverse mean velocity was over predicted in the wake by as much as 50%.

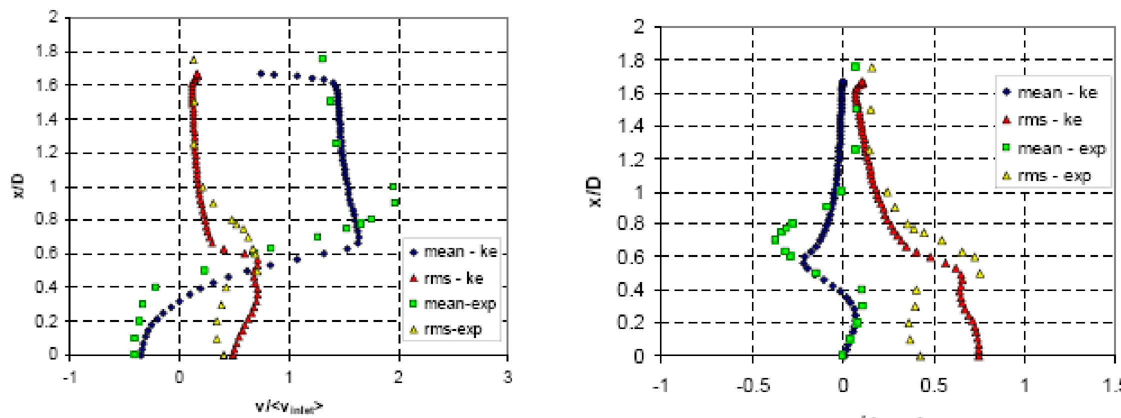

Figure 4-2 Experimental and URANS Simulation Data for Re = 55,000 and z/D = 0.5

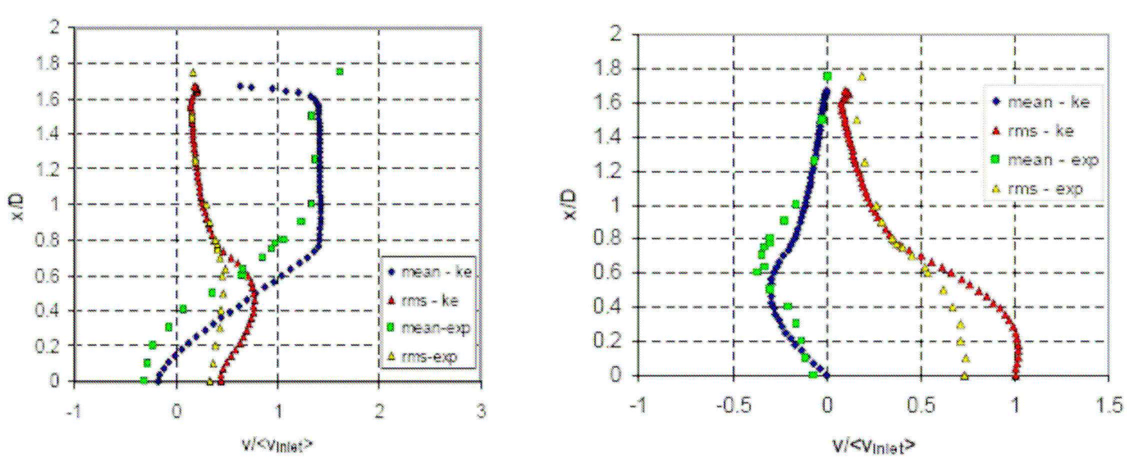

Figure 4-3 Experimental and URANS Simulation Data for Re = 55,000 and z/D = 1.0

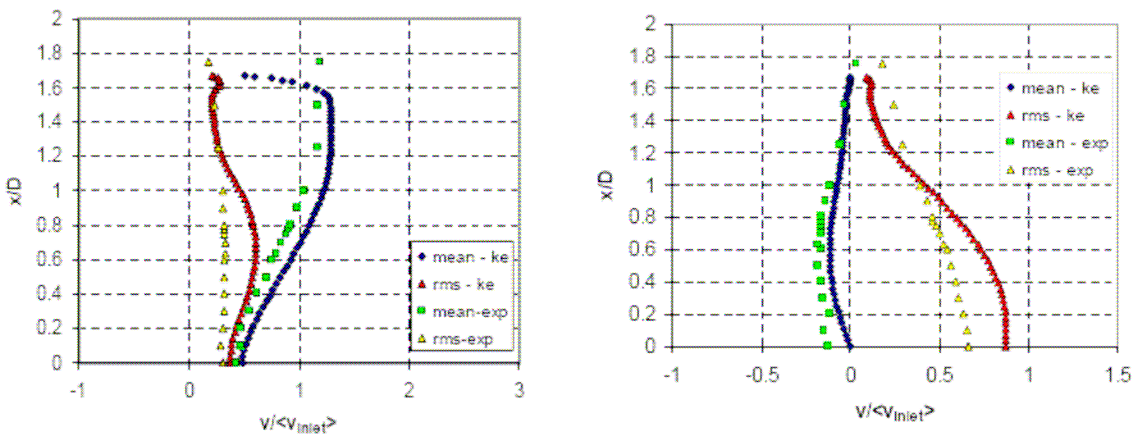

Figure 4-4 Experimental and URANS Simulation Data for Re = 55,000 and z/D = 2.0

The reported URANS simulation data used the k-epsilon model for the sub-grid turbulence. The k-epsilon model assumes the turbulence is homogenous and isotropic. For this assumption, turbulent production is assumed equal to dissipation. In the wake of a bluff body large vortices are generated. Production also occurs due to the effect of the boundary layer creating a shed shear layer. In both cases the production in these regions outpaces dissipation. In these regions the homogenous and isotropic assumptions are no longer valid thus the model does not predict the turbulence as well

5 LEAN BLOWOUT

Previously (Kiel et al. 2006) lean blowout was reported for both an open and closed v-gutter flame holders. Figure 5-1 depicts the e previously reported data.

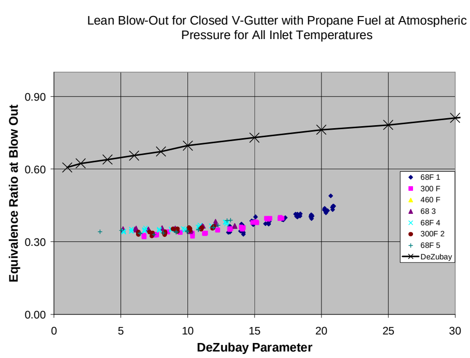

Figure 5-1 Previously Reported LBO for v-gutter Flame Holder (Kiel et al. 2006)

Added to the figure is the lean blowout equivalence ratio predicted by DeZubay correlation. The previous experimental data lies significantly below the prediction by DeZubay. Previously it was thought that the fuel and air in the rig were very well mixed.

Extinction data were compared to that of Zabetakis (1965), and Coward and Jones (1952). In their work they reported the extinction equivalence ration for premixed propane and air in the range of 0.6-0.7 depending on the inlet temperature of the propane. Ballal and Lefebvre (1979) also report similar extinction limits for the inlet conditions of the range taken in this experiment. With these three sets of data it was concluded that the fuel and air were not as well mixed as previously thought.

Detailed measurements of the fuel and air were measured to determine the level of mixedness of the fuel and air. Figures 5-2, 5-3 and 5-4 are plots of fuel air distribution for three different locations in the experimental apparatus at the lip of the flame holder. The first is parallel to the axis of the flame holder

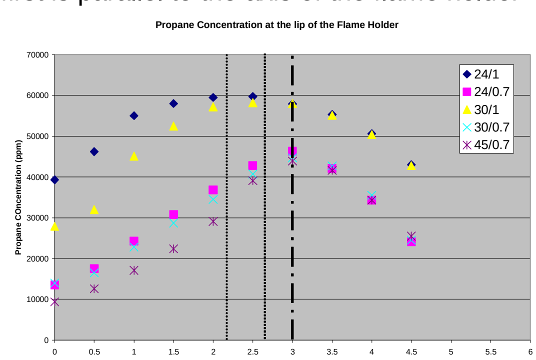

Figure 5-2 Measured Horizontal Fuel Air Distribution of the Improved Fuel Injection Configuration

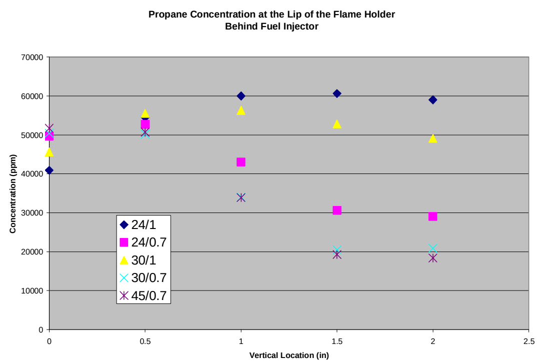

Figure 5-3 Measured Fuel Air Distribution of the Improved Fuel Injection Configuration Behind Fuel Injector

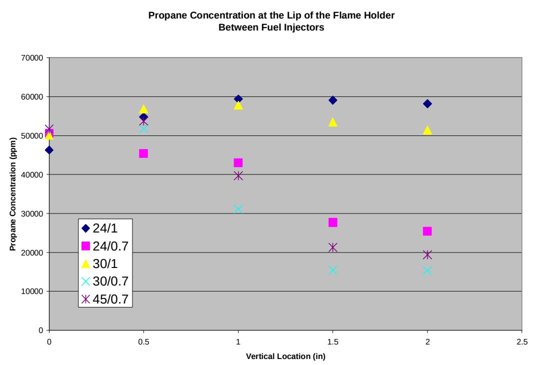

Figure 5-4 Measured Fuel Air Distribution of the Improved Fuel Injection Configuration Between Fuel Injectors

1.0 inches from the top wall. The second traverse is vertical to the flame holder behind the second fuel injector. The third is a traverse vertical to the flame holder in between the second and third fuel injectors. holder and the wall of the test article. The figures depict the fuel concentration for 20,000, 20,000, and 45,000 Reynolds number for Equivalence Rations of 1.0 and 0.7. For both the Stoichiometric cases and the lean blowout cases the fuel distribution across the flame holder was parabolic and centered. Vertically the fuel was evenly distributed at the equivalence ratio of 1.0 and was outward peaked for the equivalence ratio near lbo.

Lean blowout were taken for a v-gutter, square, and circular cylinder with the new fuel air distribution. Data were taken at atmospheric conditions over a range of Reynolds numbers from 10,000 to 50,000. Figure 5-4 depicts the lean blowout for data for all of the flame holders. Instead of plotting the data vs Reynolds number, it is plotted here against the DeZubay correlation parameter (DeZubay 1955, Kiel, 2006) Also plotted on the figure is the equivalence ratio at blow out predicted by the DeZubay correlation, the

Figure 5-4 Measured and Predicted Lean Blow Out for 3 Bluff Body Flame Holders

black line. The equivalence ratio at blow out agree much better with Dezubay. The equivalence ratio at blow out is also in the range reported by Zabetakis (1965), Coward and Jones (1952)., and Ballal and Lefebvre (1979).

Figure 5-5 zooms in on the data plotted in Figure 5-4. Upon initial examination of the data the lean blowout is insensitive to the geometry of the flame holder. Upon further investigation it is noted that the lean blow out all occur at equivalence ratios higher than that predicted by Dezubay. From correlation parameter between 5 and 12, the data differ less than 3%. For correlation parameter greater than 12, the difference increases to 12%.

The increase in the experimental data relative to the predicted can be explained with further scrutiny of the measured propane

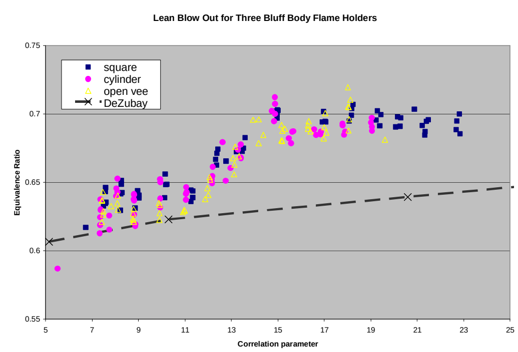

Figure 5-5 Close In View of Measured and Predicted Lean Blow Out for 3 Bluff Body Flame Holders

plots, Figure 5-3, and 5-4. In these figures the concentration of the propane fuel changes near the flame holder as the inlet mass flow increases. Near the flame holder the fuel air ratio changes as much as 50%, while remaining steady closer to the wall. This change in fuel air distribution is probably the cause of the change in lbo as correlation parameter increases.

6 HIGH SPEED IMAGES

High speed images were taken of the three flame holders at several different conditions. For each flame holder the inlet conditions were atmospheric. Three different Reynolds numbers were imaged, 20,000, 30,000, and 40,000. For each flame holder and Reynolds number, images were taken at an equivalence ratio of 1.0 and taken just prior to blowout.

Figure 6-1 is an instantaneous image of, from top to bottom, the circular cylinder, square cylinder, and v-gutter flame holders. The Reynolds number for the image was 20,000. The equivalence ratio was 1.0. In this image the three flames are very different. In the wake of the cylinder the flame is anchored in the shear layer being shed from the bluff body boundary layer and there are large flame vortices being shed behind the cylinder. For the square cylinder and the v-gutter the flame is anchored in the shear layer shed from the bluff body boundary layer. There little vortex motion in the wake of these flame holders.

Figures 6-2, and 6-3 are instantaneous images of, from top to bottom, the circular cylinder, square cylinder, and v-gutter flame holders. The Reynolds number s are 30,000, and 40,000 respectively. In both cases the equivalence ratio was 1.0. In figure 6-2 the wake of the cylinder is still dominated by large vortices. In figure 6-3, however the wake of the cylinder changes dramatically. It is no longer dominated by large vortices, and instead seems to be only shear driven.

Figure 6-1, High Speed Images of the Circular Cylinder, Square Cylinder and V-Gutter at Re = 20,000, Equivalence Ratio = 1.0

Understanding the vortex shedding patterns in these three different flames can be achieved through a discussion of the forces that dominate the fluid motion. For a circular cylinder the point at which the boundary layer separates is controlled by Reynolds number. As the Reynolds number increases the momentum forces become more dominant relative to viscous forces. Because of this the separation point moves further and further forward on the surface of the cylinder. The

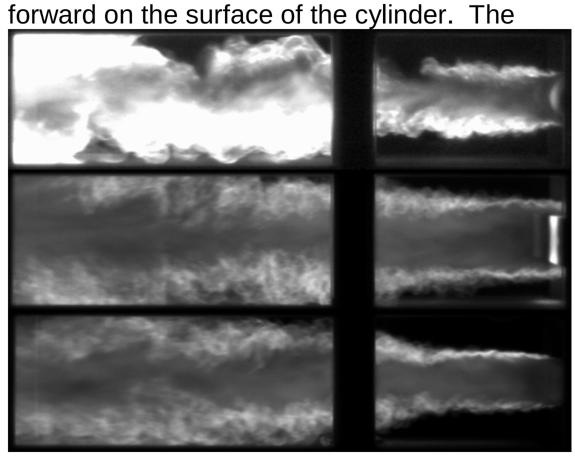

Figure 6-2, High Speed Images of the Circular Cylinder, Square Cylinder and V-Gutter at Re= 30,000, Equivalence Ratio = 1.0

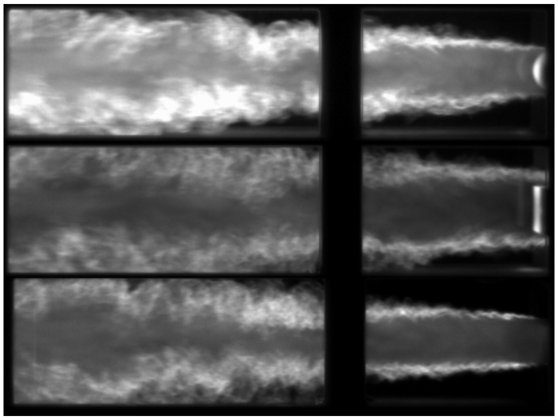

Figure 6-3, High Speed Images of the Circular Cylinder, Square Cylinder at Re = 40,000, Equivalence Ratio = 1.0

vortices in the wake also become smaller and the wake becomes more turbulent as the momentum of the oncoming air increases. For the square cylinder and v-gutter the boundary layer initiates at the leading edge of the flame holder and does not move as a function of the momentum of the incoming gas.

When combustion is considered a third force becomes relevant, the baroclinic torque associated with the density rise across the flame. For the square and v-gutter the dominant forces in the flow are the momentum and baroclinic forces, both of which tend to generate smaller vortices and suppress the formation of viscous driven Kanman Street Vortices. The circular cylinder, on the other hand, is first dominated by viscous forces, producing large vortices in the flame wake. As the velocity is increased the momentum forces increase and at Reynolds number of 40,000 the momentum and baroclinic forces dominate the flow, suppressing the viscous driven large vortices in the wake.

Different vortex dynamics occur near blowout. Figures 6-4, 6-5, and 6-6 are instantaneous images of, from top to bottom, the circular cylinder, square cylinder, and v-gutter flame holders. The Reynolds numbers are 20,000, 30,000, and 40,000 respectively. The images were taken just before the flame blew out. These images are very different from those at stoichiometric conditions, Figures 6-1 through 6-3. In all of the images of the flame near blow out, for all of the geometries and Reynolds numbers, the images look similar. In each the flame is dominated by large vortex motion just before blowout.

In figures 5-4 and 5-5 blowout of the three different flame holders was independent of geometry. At first this was counter intuitive. In Figure 4-1 it was seen that the non-reacting vortex shedding was quite different for the three different flame holders. Further the high speed images at stoichiometric conditions indicated that the circular cylinder had very diffident flame motion then the other two bluff bodies. These differences in the vortex motion would lead one to believe that the blowout should depend on geometry.

Figure 6-4, High Speed Images of the Circular Cylinder, Square Cylinder and V-Gutter at Re = 20,000, Near Extinction

Figures 6-4 through 6-6, though, depict very similar flame structure at blowout, regardless of geometry. Experiments were conducted in the 1950's at then NACA for a wide variety of flame holders, Henzel and Bryant (1954), Nakanishi et al. (1953), and Williams et al. (1956). In this research 14 different flame holder configurations were

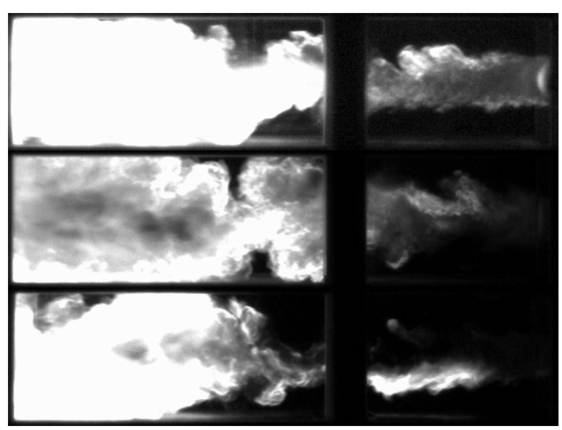

Figure 6-5, High Speed Images of the Circular Cylinder, Square Cylinder and V-Gutter at Re = 30,000, Near Extinction

Figure 6-6, High Speed Images of the Circular Cylinder, Square Cylinder and V-Gutter at Re = 40,000, Near Extinction

tested over a wide range of inlet parameters. The conclusions were that the flame extinction was more sensitive to the approach velocity and the width of the flame holder and less sensitive to the actual geometry.

8 CONCLUSIONS

In the previous paper (Kiel 2006) it was asserted that the large vortices were a major driver in extinction. Those assertions are further supported here. It is concluded that the vortex dynamics and not geometry is the dominant mechanism for bluff body flame extinction. This conclusion is supported by the high speed images and figure 5-4. First, a review of Figure 5-4 and the NACA data support the assertion that extinction is insensitive to geometry.

The high speed images also support this assertion. At stoichiometric conditions the square and v-gutter are dominated by shear layer stabilized flames. The circular cylinder is dominated by both shear layer stabilization and by large vortices. For these flames the shear layer acts to increase the temperature of the reactants as they are convected into the flame zone. The temperature rise associated with the flame also produces baroclinic forces which, with momentum, dominate the flow. Even for the circular cylinder some large scale vortices that were present at 20,000 and 30,000 Reynolds number. These were eventually suppressed at Reynolds number 40,000 when momentum and baroclinic forces are sufficient to dominate.

Near extinction the stoichiometry, thus the flame temperature is reduced. This reduction in flame temperature reduces the baroclinic forces associated with the flame. The reduction in baroclinic forces is sufficient for large vortices to form in the flame regardless of the geometry of the flame holder. The large vortices contribute to extinction by increasing the strain on the surface of the flame. From the images it is also evident that cold reactants are also entrained into the wake as the large flame structures are shed.

9 RECOMMENDATIONS

Continued research is required to support the conclusions drawn. Being developed are algorithms that post process the high speed images. These algorithms will quantify the flame strain. Also planned are experiments in the reacting flow using LDV and Particle Image Velocimetry (PIV). These will further quantify the strain in the wake of the flame holders over the range of test conditions. Tunable Diode LASER and CARS Experiments are also planned to measure the time varying temperature in the wake. These measurements combined will ascertain the effect the large vortices have on reactant temperature.

The experimental data and phenomenology ascertained here are also key to all types of model validation. A parallel effort is under way to incorporate the phenomenology with CFD to develop a methodology to assess flame stability with a reduced order model.

10 REFERENCES

Ballal, D., and Lefebvre A., 1979, “Weak Extinction Limits for Flowing Turbulent Mixtures”, Journal of Engineering and Power, 101, p 343-348.

Blevins R., 1977, Flow Induced Vibrations, Van Nostrand Reinhold Co., NY NY, ISBN 0-442-20828-6.

Blevins R., 1985, “The Effect of Sound on Vortex Shedding from Cylinders”, *J. Fluid Mech*., Vol. 161, pp. 217-237.

Coward, H. F., and Jones, G. W., 1952 "**Limits of Flammability of Gases and Vapors**,".
U. S. Bureau of Mines Bulletin 503.

DeZubay, E. A., 1950, “Characteristics of Disk-Controlled Flame,” *Aero Digest*, pp. 54-57.

Erickson, R., Soteriou, M., and Prashant, M., 2006, “The Influence of Temperature Ratio on the Dynamics of Bluff Body Stabilizee Flames”, AIAA 2006-753.

Fureby, C., 2006, “A Comparison of Flamelet LES Models for Premixed Turbulent Combustion”, AIAA 2006-155.

Henzel, J., and Bryant, L., 1954, “Investigation of Effect of Number and Width of Annular Flame-Holder Gutters on Afterburner Performance”, NACA RM E54C30.

Kiel et al., 2006, “Non-reacting and Combusting Bluff Bodies in Cross Flow”, AIAA 2006-5234.

King, C. R., 1957, “A Semi Empirical Correlation of Afterburner Combustion Efficiency and Lean-Blowout Fuel-Air-Ratio with Several Afterburner Inlet Variables and Afterburner Lengths,” NACAE57RMF26.

Mehta, P.G., and Soteriou, M.C., 2003, “Combustion Heat Release Effects on the Dynamics of Bluff Body Stabilized Premixed Reacting Flows”, *AIAA 2003-0835*.

Nakanishi, S., et al., 1953, “An Investigation of Effects of Flame-Holder Gutter Performance”, NACA RM E53J14.

Norburg, C., 1993, “Flow Around Rectangular Cylinders, Pressure Forces and Wake Frequencies”, J. Wind Eng. Ind. Aerodynamics, 19, p 187-196.

Ozowa, R. I., 1971, “Survey of Basic Data on Flame Stabilization and Propagation for High Speed Combustion Systems”, AFAPL-TR-70-81.

Porumbel, I., and Menon, S. 2006, “Large Eddy Simulation of a Body Stabilized Premixed Bluff Flame:, AiAA 2006-0152.

Prince, W., et al., 1956, “Full-Scale Evaluation of Some Flameholder Design Concepts for High-Inlet-Velocity Afterburners”, NACA RM E56D10.

Roshko, A., 1954, “On the Drag and Shedding Frequency Two Dimensional Bluff Bodies”, NACA TN 3169.

Roshko, A., 1954, “On the Development of Turbulent Wakes From Vortex Streets”, NACA Report 1191.

Taylor, I, and Vezza, M., 1999, “Prediction of Unsteady Flow Around Square and Rectangular Section Cylinders Using Discrete Vortex Method”, J. Wind Eng. Aerodynamics, 82, p 247-269.

Younger G., Gabriel, D., and Mickelsen, W., 1951, Experimental Study of Isothermal Wake-Flow Characteristics of Various Flame Holder Shapes”, NACA RM E51K07.

Zukoski, E., 1954, “Experiments Concerning the Mechanism of Flame Blowoff From Bluff Bodies,” Thesis, California Institute of Technology.

Zukoski, E., and Marble, F., 1955, “The Role of Wake Transition in the Process of Flame Staboilization on Bluff Bodies”, AGARD Combustion Research and Reviews, 167-180.

Zabetakis, M. G., 1965, “Flammability Characteristics of Combustable Gases and Vapors”, US Bureau of Mines Bulletin 627.